Effect of Fatigue Loading on The Functional Integrity of Intervertebral Disc

Jaw-Lin Wang（王兆麟）, Wang-Chu Chen（陳旺初）
國立台灣大學　醫學院暨工學院 醫學工程學研究所
E-mail: jlwang@ntu.edu.tw

ABSTRACT

Epidemiological studies showed the repetitive activity as a risk factor for back pain. Most of the fatigue failures of spinal column are the consequence of disc dysfunction. The biomechanical function of disc is to hold the intradiscal pressure, hence maintaining the stiffness of disc and providing the stability of motion segment. The information of the effect of fatigue loading on the disc integrity is important for clarifying the risk factor of back pain. The objective of this study was to assess the changes of functional integrity of intervertebral disc post fatigue loading. An in vitro biomechanical study using porcine spine specimen was designed. Quantitative discomanometry (QD) test was applied pre and post fatigue. The characteristic pressures, volumes and slope of pressure-volume curve of the QD test were analyzed. The results showed the fatigue loading decreased the functional integrity of intervertebral disc. The disc was at higher risk of injury following fatigue loading.
Key Words: intervertebral disc, intradiscal pressure, repetitive loading

INTRODUCTION

Occupations that required higher cumulative spinal compression and shear forces often led to low back pain (LBP) problems [1]. Epidemiological studies suggested highly repetitive activities as a risk factor for LBP [2, 3]. For example, the exposure of whole body vibration was proved to be a risk factor for occupational LBP [4, 5]. The fatigue failure of disc often leads to the acceleration of the degenerative processes and development of low back disorders. The mechanism of disc fatigue failure is a complex process. The frequent bending and lifting often led disc protrusion [6, 7]. The sub-maximal cyclic loading will induce disc micro failures [8] hence making the spine unstable [9].

The fatigue failure of motion segment can be observed at the vertebral body (VB) and endplate due to axial compressive cyclic loading [3, 9, 10]; at the anulus fibrosus (AF) due to flexion cyclic loading [11]; and at the endplate, facet, AF and capsular ligament

due to torsion cyclic loading [12]. The injury site of spinal fatigue failure was observed in many places within the motion segment. However, the fatigue failure of motion segment generally started from the dysfunction of disc [13-15].

One of the biomechanical functions of disc is to absorb the force transmitted from the ground reaction. The disc is a viscoelastic structure consisting of a nucleus pulposus (NP) surrounded by AF. The AF is an elastic laminated fibrous structure that holds the intradiscal pressure (IDP), hence providing the capability of absorbing force [16]. The micro failure of AF due to fatigue loading was likely to damage the disc integrity. However, the quantitative links between disc integrity and fatigue loading was inadequately studied. To address these questions, the study investigated the functional integrity of disc following fatigue loading. Quantitative information of the effect of fatigue loading on disc integrity will be helpful in defining the injury potential of disc.

MATERIAL AND METHOD

Specimen Preparation. Three-unit-motion-segment (T2-T5, T6-T9) of fresh porcine thoracic specimens were harvest from 6-month-old swine. The discs were rated Grade 1 criteria defined by Galante [17] **(Figure 1)**. Each specimen was carefully cleaned of muscle tissue. The specimens were mounted at both ends, i.e., the proximal half of cranial vertebra and the distal half of caudal vertebra, using quick setting epoxy. The specimens were placed in double plastic bags and frozen at –20º C for storage. Before experiments, the specimens were removed from freezer and kept in room temperature for 6 hours. The specimens were wrapped with gauze and saline during the experiments. The size of tested porcine thoracic disc was close to the size of human one [18, 19] **(Table 1).**

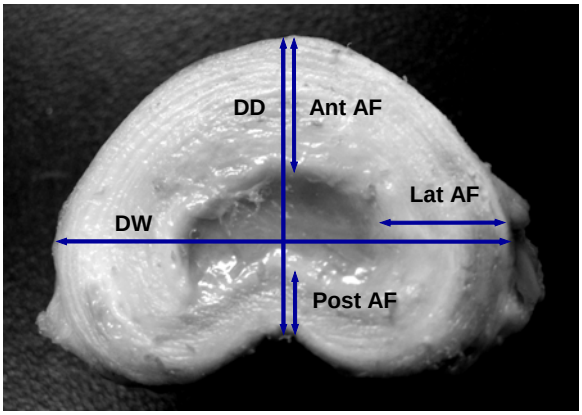

DW: Disc Width
DD: Disc Depth
Ant AF: Thickness of Anterior AF
Lat AF: Thickness of Lateral AF
Post AF: Thickness of Posterior AF

Figure 1. The width, depth and height of disc and thickness of anulus fibrosus of porcine thoracic disc.

Table 1. Dimensions (mm) of Porcine and Human Discs.

	Porcine thoracic disc	Human thoracic disc
Disc height	5.2 (0.3)	6.6 (1.4) [19]
Disc width	34.1 (2.4)	*EPWu=28.6 (4.7), EPWl=31.0 (5.3) [18]
Disc depth	22.5 (0.9)	*EPDu=26.2 (4.6), EPDl=27.3 (4.4) [18]
Ant AF	7.3 (0.9)	N.A.
Lat AF	7.4 (0.5)	N.A.
Post AF	4.1 (0.3)	N.A.

Data are mean (standard deviation).

*Data are based on the measurement of endplate.

EPWu: Upper endplate width, EPWl: Lower endplate width,

EPDu: Upper endplate depth, EPDl: Lower endplate depth, N.A.: Not Available

Quantitative Discomanometry (QD) Apparatus. The QD technique [20-23] was used to measure both the injected fluid volume and the developed hydrostatic pressure within the disc to quantify the disc functional integrity. The QD apparatus was composed of a spinal needle, a high-pressured syringe, a programmable x-table, a pressure transducer and a linear potentiometer (for volume measurement) **(Figure 2)**. The pressure limit of the home-made QD apparatus was 5 MPa and the linear range of pressure-volume curve was 4.5 MPa. This QD apparatus was able to inject 1 ml fluid. In the pilot study, most the pressure leaked within 0.1 ml and saturated less than 0.5 ml. We set the 0.5 ml as the injection volume. The injection rate was fixed at 0.5 ml/min. The 22 G spinal needle with 90 mm length was carefully placed in the center of the disc through lateral site of disc with the help of a plastic stopper/indicator.

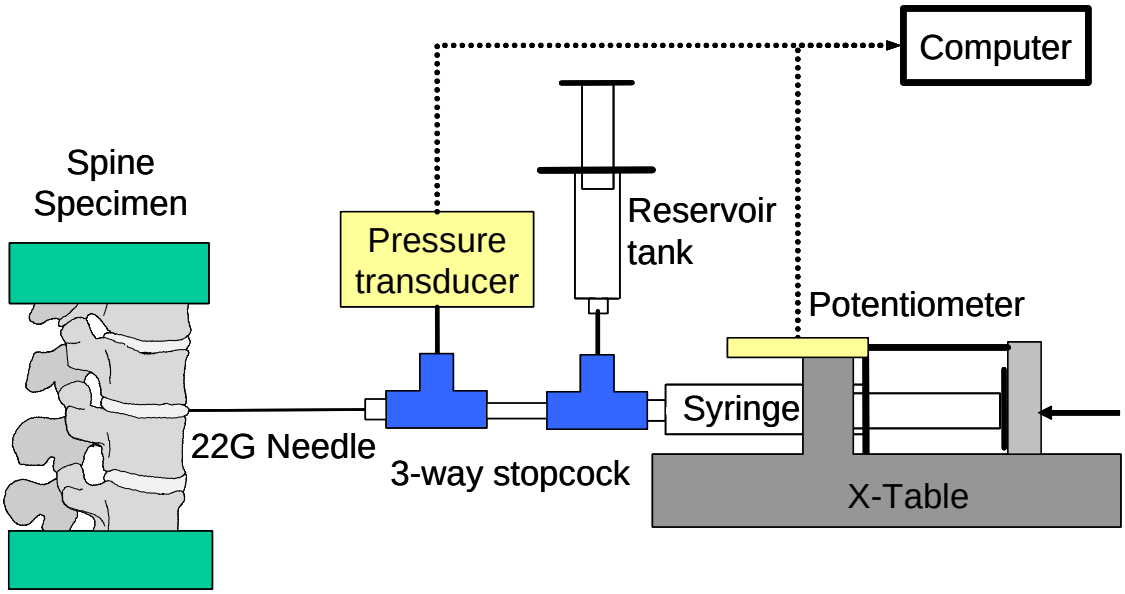

Figure 2. Quantitative discomanometry (QD) apparatus. The QD apparatus was composed of a spinal needle, a high-pressured syringe, a programmable x-table, a pressure transducer for pressure measurement, a linear potentiometer for volume measurement and a computer for data acquisition.

Fatigue Loading Apparatus. A vibrator composed of two eccentric rotors and one motor was mounted into the impactor of the impact testing apparatus to create the fatigue loading **(Figure 3)**. The fatigue loading was produced by the rotation of two counter-rotated eccentric rotors driven by a motor. The vibration was transmitted to the specimen through the impounder. The specimen was vertically loaded on top of the anterolateral site of specimen using an eccentric wedge (4 cm from the center of the vertebrae) to mimic the combination of axial compression and lateral flexion **(Figure 3)** [24]. A load cell (AMTI MC6-6-4000, Advanced Mechanical Technology, Inc., Watertown, MA, USA) was placed under the specimen to record the resultant forces and moments of the specimen. The root mean squared averaged axial loading of cyclic loading was 425 N (670 N maximum and 270 N minimum), and the flexion was 17 Nm (27 Nm maximum and 11 Nm minimum). The loading frequency was 5 Hz and the loading period was five hours. In total, 90,000 cycles of loading were applied.

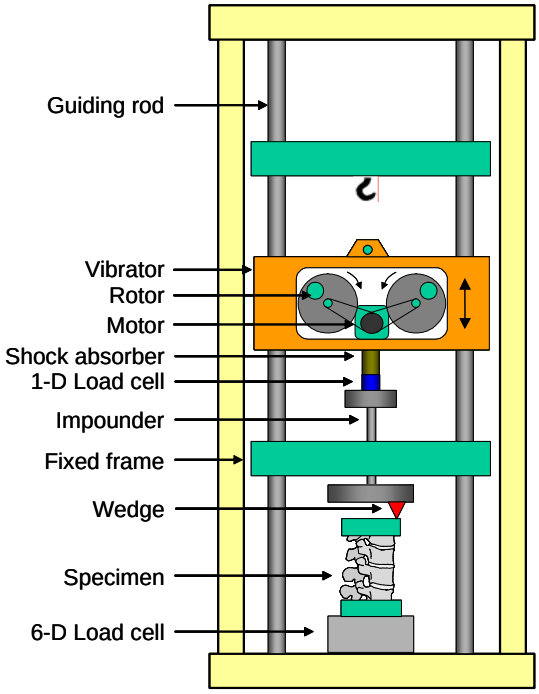

Figure 3. Fatigue testing apparatus. The fatigue loading, generated by the vibration of vibrator, was transmitted to the specimen through impounder. A wedge was applied on the top of the specimen and anterolaterally eccentric to the center of vertebra to create a compressive loading combined with anterolateral flexion motion.

Experimental Protocol. Two specimens were used to confirm the morphological changes post fatigue by cross-sectional dissected disc photography. Ten intact discs were tested by QD apparatus, and another ten discs (the middle disc of 3-unit-motion-segment specimen) were tested by QD apparatus post fatigue.

Data Analysis. The independent variable manipulated in the experiment was the fatigue loading (pre and post fatigue). The dependent variables were the QD parameters. The QD parameters included the intrinsic pressure, leakage pressure and volume, saturate pressure and volume, steady-state pressure, and slope between intrinsic and leakage pressure **(Figure 4)** [21]. The intrinsic pressure was the disc pressure before injection. The leakage pressure and volume were the pressure and volume of the linear threshold of pressure-volume curve. The saturate pressure and volume were the pressure and volume of the maximum pressure during the injection. The steady-state pressure was defined as the pressure when the injected volume was 0.5 ml.

Statistical Analysis. The independent sample t-test was used to detect the statistical difference of QD parameters between pre and post fatigue loading. The tests were considered to be significant at α=0.05.

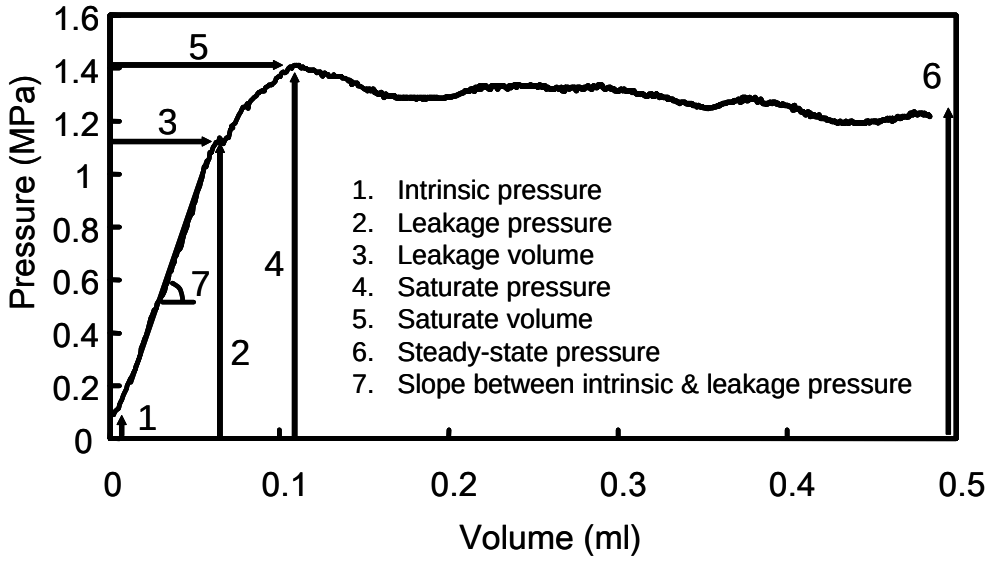

Figure 4. Schematics of a pressure-volume curve obtained using QD apparatus.

RESULTS

Morphological Observation. No visible protrusion of NP was observed post fatigue. A solution of black ink dye was injected into the center of the discs before fatigue loading. After the fatigue loading, the photography of cross-sectional dissected disc showed the NP compressed the AF of the posterolateral side **(Figure 5)**.

QD parameters. All QD parameters, except the saturate volume, significantly decreased post fatigue **(Table 2)**. Higher magnitude of QD pressure represents better disc integrity. The leakage pressure, saturate pressure and steady-state pressure of discs were above the machine's limit (5 MPa) pre fatigue, and dropped to 1.7, 2.3 and 2.2 MPa post fatigue. The slope between intrinsic and leakage pressure corresponded to the elasticity of the AF ring. The slope was 44.6 MPa/ml pre fatigue and decreased to 27.1 MPa/ml post fatigue.

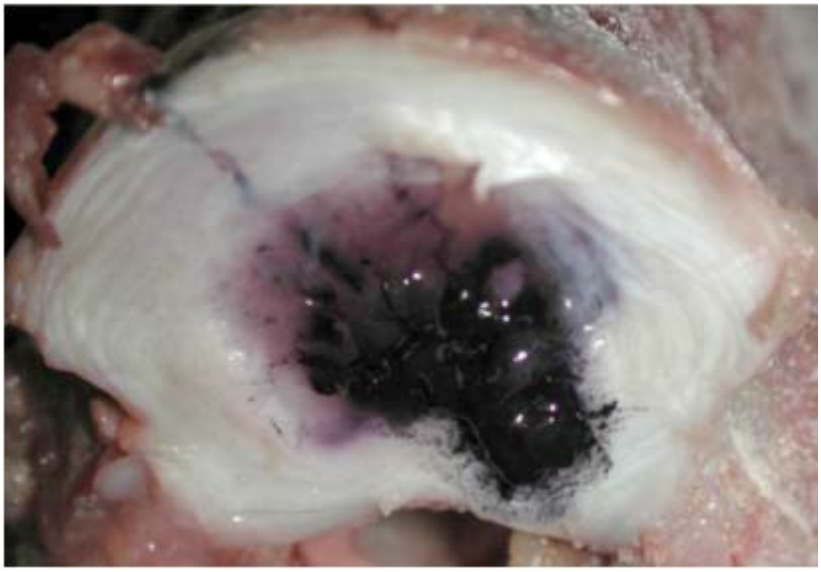

Figure 5. Photograph of a sectioned disc post fatigue load. After axial loading combine with left anterolateral flexion fatigue loading, the nucleus pulposus protruded toward the right posterolateral side of the disc.

Table 2. Comparison of QD Parameters Pre and Post Fatigue Loading.

	Pre fatigue	Post fatigue	P-value
Intrinsic pressure (MPa)	0.14 (0.06)	0.06 (0.03)	0.003
Leakage pressure (MPa)	*3.92 (0.01)	1.71 (1.16)	0.000
Saturate pressure (MPa)	*4.99 (0.09)	2.28 (1.20)	0.000
Steady-state pressure (MPa)	*4.99 (0.17)	2.24 (1.25)	0.000
Leakage volume (ml)	0.14 (0.06)	0.08 (0.06)	0.041
Saturate volume (ml)	0.22 (0.08)	0.16 (0.08)	0.072
Slope (MPa/ml)	44.6 (20.6)	27.1 (9.80)	0.030

Data are Average (Standard Deviation).

* Exceed machine limit.

DISCUSSION

The outcome of biological structure (e.g. spine) post fatigue loading was complicated and difficult to compare among different researches. It was because the type and magnitude of fatigue loading was not clearly defined and the loading conditions were not consistent. The fatigue test of engineering materials was categorized into the high cycle fatigue and the low cycle fatigue. The differentiation between the high cycle and

low cycle fatigue loading in spine biomechanics was less discussed. It is tentatively suggested the two types of fatigue loading can be divided by the activities that spine experienced. For example, the low cycle fatigue may simulate the loading during repetitive lifting of moderate to heavy weight (3 Nm for 9,000 cycles [25], 500 N to 3150 N, for 8253, 3257 and 263 cycles at 0, 22.5, and 45 degree flexion [26, 27], 1,472 N (mean) for 6,000 cycles [24], and 3,076 N (mean) for 9,600 cycles [28]). The high cycle fatigue may simulate the loading during a vibratory environment without excessive bearing (260 N (mean) for 86,400 cycles [29]). The loading magnitude of 425 N (mean) for 90,000 cycles used in current study can be attributed to the high cycle fatigue loading condition. Differentiating type of fatigue loading help synthesize experimental results.

The current study created an in vitro mechanically degenerated disc, but not the chemical or aging degenerated disc [30-32]. An aging degenerated disc would yield lower swelling stress [30], higher tensile and compressive strain [13], and higher leakage volume [31]. We did not find the increased leakage or saturate volume post fatigue. On the contrary, we found a minor decreased leakage and saturate volume post fatigue. The process of current mechanical degeneration did not enlarge the volume of NP, while the process of aging degeneration did.

The porcine spine/disc is a good animal model to simulate human spine/disc. The loading axis of the quadruped spine is mainly along its long axis, just like human spine [33]. The porcine spine is analogue to human spine in terms of anatomical, geometrical and functional characteristics [29, 34]. In addition, the physical circumstance of a 6-month old porcine disc can represent the one of human mature and health disc. However, limitations of using the porcine spine should be addressed. The current study applied vertical loading along the long axis of motion segment. The anterior porcine facet joint (analogous to the superior facet joint in human spine) is a hook-like process and the human facet joint is a straight process. This geometric difference should increase the load sharing percentage of facet joint during anteroposterior and lateral shear loading. The increased load sharing percentage during axial loading is not clear and worth of further study.

This study found that the saturate pressure of porcine intact disc was higher than 5 MPa (machine's limit) pre fatigue and dropped to 2 MPa post fatigue. The saturate pressure of an intact bovine disc was 18 MPa [35]. The saturate pressure of intact porcine disc should also be within this range. The saturate pressure of disc secondary to burst fracture was 0.3 MPa [23] and the saturate pressure of degenerated human disc was from 0.8 MPa to 1.3 MPa [36]. The current fatigue loading did not create a significant injury as the burst fracture or degeneration did. However, the fatigue loading would increase the

risk of disc leakage even with regular activities, since the IDP under regular daily activities can be up to 1.6 MPa [37] to 2 MPa [38, 39].

This study showed that the fatigue loading decreased the functional integrity. The disc was at higher risk of injury post fatigue even at mild loading. Two concerns should be addressed for the application of the quantitative data. First, the inherent mechanical strength of healthy porcine disc was stronger than the one of degenerated human disc. Second, the human spine experienced 10,000 to 20,000 cycles of loading per day. A 90,000 cycles of repetitive loading at 425 N (mean) without rest was a rigorous loading test for spine/disc. The in vitro fatigue experiments showed both the reversible [40] and irreversible [41] changes of disc mechanical properties. Establishing the index of critical fatigue loading for human disc is imperative for preventing permanent injury of disc. This study created a starting reference point for future study.

ACKNOWLEDGEMENT

Graduate students, Ke-Yong Wang, Chun-Kai Chaing and Chia-Chun Hsu, helped building the testing apparatus. Funding of the research came from National Science Council, Taiwan (NSC 92-2320-B-002-091, NSC 94-2320-B-002-035) and National Health Research Institute, Taiwan (NHRI-EX95-9425EI).

REFERENCES

[1] Kumar S. Cumulative load as a risk factor for back pain. Spine 1990; 12: 1311-6.

[2] Marras WS, Lavender SA, Leurgans SE, Fathallah FA, Ferguson SA, Allread WG, Rajulu SL. Biomechanical risk factors for occupationally related low back disorders. Ergonomics 1995; 2: 377-410.

[3] Marras WS, Parakkat J, Chany AM, Yang G, Burr D, Lavender SA. Spine loading as a function of lift frequency, exposure duration, and work experience. Clin Biomech (Bristol, Avon) 2006; 4: 345-52.

[4] Wilder DG, Pope MH. Epidemiological and aetiological aspects of low back pain in vibration environments - an update. Clin Biomech (Bristol, Avon) 1996; 2: 61-73.

[5] Kumar A, Varghese M, Mohan D, Mahajan P, Gulati P, Kale S. Effect of whole-body vibration on the low back. A study of tractor-driving farmers in north India. Spine 1999; 23: 2506-15.

[6] Kelsey JL, Githens PB, Walter SD, Southwick WO, Weil U, Holford TR, Ostfeld AM, Calogero JA, O'Connor T, White AA, 3rd. An epidemiological study of acute prolapsed cervical intervertebral disc. J Bone Joint Surg Am 1984; 6: 907-14.

[7] Kelsey JL, Githens PB, White AA, 3rd, Holford TR, Walter SD, O'Connor T, Ostfeld

AM, Weil U, Southwick WO, Calogero JA. An epidemiologic study of lifting and twisting on the job and risk for acute prolapsed lumbar intervertebral disc. J Orthop Res 1984; 1: 61-6.
[8] Lafferty JF, Winter WG, Gambaro SA. Fatigue characteristics of posterior elements of vertebrae. J Bone Joint Surg Am 1977; 2: 154-8.
[9] Liu YK, Njus G, Buckwalter J, Wakano K. Fatigue response of lumbar intervertebral joints under axial cyclic loading. Spine 1983; 8: 857-65.
[10] Hansson TH, Keller TS, Spengler DM. Mechanical behavior of the human lumbar spine. II. Fatigue strength during dynamic compressive loading. J Orthop Res 1987; 4: 479-87.
[11] Adams MA, Hutton WC. Gradual disc prolapse. Spine 1985; 6: 524-31.
[12] Liu YK, Goel VK, Dejong A, Njus G, Nishiyama K, Buckwalter J. Torsional fatigue of the lumbar intervertebral joints. Spine 1985; 10: 894-900.
[13] Tsantrizos A, Ito K, Aebi M, Steffen T. Internal strains in healthy and degenerated lumbar intervertebral discs. Spine 2005; 19: 2129-37.
[14] Zhao F, Pollintine P, Hole BD, Dolan P, Adams MA. Discogenic origins of spinal instability. Spine 2005; 23: 2621-30.
[15] Pollintine P, Dolan P, Tobias JH, Adams MA. Intervertebral disc degeneration can lead to "stress-shielding" of the anterior vertebral body: a cause of osteoporotic vertebral fracture? Spine 2004; 7: 774-82.
[16] Lee CK, Kim YE, Lee CS, Hong YM, Jung JM, Goel VK. Impact response of the intervertebral disc in a finite-element model. Spine 2000; 19: 2431-9.
[17] Galante JO. Tensile properties of the human lumbar annulus fibrosus. Acta Orthop Scand 1967; Suppl 100:1-91.
[18] Panjabi MM, Takata K, Goel V, Federico D, Oxland T, Duranceau J, Krag M. Thoracic human vertebrae. Quantitative three-dimensional anatomy. Spine 1991; 8: 888-901.
[19] Chanchairujira K, Chung CB, Kim JY, Papakonstantinou O, Lee MH, Clopton P, Resnick D. Intervertebral disk calcification of the spine in an elderly population: radiographic prevalence, location, and distribution and correlation with spinal degeneration. Radiology 2004; 2: 499-503.
[20] Panjabi M, Brown M, Lindahl S, Irstam L, Hermens M. Intrinsic disc pressure as a measure of integrity of the lumbar spine. Spine 1988; 8: 913-7.
[21] Fye MA, Southern EP, Panjabi MM, Cholewicki J. Quantitative discomanometry: technique and reproducibility in vitro. J Spinal Disord 1998; 4: 335-40.
[22] Southern EP, Fye MA, Panjabi MM, Patel TC, Cholewicki J. Disc degeneration: a

human cadaveric study correlating magnetic resonance imaging and quantitative discomanometry. Spine 2000; 17: 2171-5.
[23] Wang JL, Panjabi MM, Kato Y, Nguyen C. Radiography cannot examine disc injuries secondary to burst fracture: quantitative discomanometry validation. Spine 2002; 3: 235-40.
[24] Aultman CD, Scannell J, McGill SM. The direction of progressive herniation in porcine spine motion segments is influenced by the orientation of the bending axis. Clin Biomech (Bristol, Avon) 2005; 2: 126-9.
[25] Goel VK, Voo LM, Weinstein JN, Liu YK, Okuma T, Njus GO. Response of the ligamentous lumbar spine to cyclic bending loads. Spine 1988; 3: 294-300.
[26] Gallagher S, Marras WS, Litsky AS, Burr D. An exploratory study of loading and morphometric factors associated with specific failure modes in fatigue testing of lumbar motion segments. Clin Biomech (Bristol, Avon) 2006; 3: 228-34.
[27] Gallagher S, Marras WS, Litsky AS, Burr D. Torso flexion loads and the fatigue failure of human lumbosacral motion segments. Spine 2005; 20: 2265-73.
[28] Adams MA, Hutton WC. The effect of fatigue on the lumbar intervertebral disc. J Bone Joint Surg Br 1983; 2: 199-203.
[29] Callaghan JP, McGill SM. Intervertebral disc herniation: studies on a porcine model exposed to highly repetitive flexion/extension motion with compressive force. Clin Biomech (Bristol, Avon) 2001; 1: 28-37.
[30] Johannessen W, Elliott DM. Effects of degeneration on the biphasic material properties of human nucleus pulposus in confined compression. Spine 2005; 24: E724-9.
[31] Brown MD, Holmes DC, Heiner AD. Measurement of cadaver lumbar spine motion segment stiffness. Spine 2002; 9: 918-22.
[32] Singh K, Masuda K, An HS. Animal models for human disc degeneration. Spine J 2005; 6 Suppl: 267S-279S.
[33] Smit TH. The use of a quadruped as an in vivo model for the study of the spine - biomechanical considerations. Eur Spine J 2002; 2: 137-44.
[34] McLain RF, Yerby SA, Moseley TA. Comparative morphometry of L4 vertebrae: comparison of large animal models for the human lumbar spine. Spine 2002; 8: E200-6.
[35] Schechtman H, Robertson PA, Broom ND. Failure strength of the bovine caudal disc under internal hydrostatic pressure. J Biomech 2005.
[36] Iencean SM. Lumbar intervertebral disc herniation following experimental intradiscal pressure increase. Acta Neurochir (Wien) 2000; 6: 669-76.
[37] Takahashi I, Kikuchi S, Sato K, Sato N. Mechanical load of the lumbar spine during forward bending motion of the trunk-a biomechanical study. Spine 2006; 1: 18-23.

[38] Wilke H, Neef P, Hinz B, Seidel H, Claes L. Intradiscal pressure together with anthropometric data--a data set for the validation of models. Clin Biomech (Bristol, Avon) 2001; S111-26.
[39] Wilke HJ, Neef P, Caimi M, Hoogland T, Claes LE. New in vivo measurements of pressures in the intervertebral disc in daily life. Spine 1999; 8: 755-62.
[40] Johannessen W, Vresilovic EJ, Wright AC, Elliott DM. Intervertebral disc mechanics are restored following cyclic loading and unloaded recovery. Ann Biomed Eng 2004; 1: 70-6.
[41] van der Veen AJ, Mullender M, Smit TH, Kingma I, van Dieen JH. Flow-related mechanics of the intervertebral disc: the validity of an in vitro model. Spine 2005; 18: E534-9.